Mechanisms regulating TGF-β and Wnt signal transduction in breast cancer

Li, Y.

Chapter 4

c-Myb enhances breast cancer invasion and metastasis through the Wnt/β-catenin/Axin2 pathway

Yihao Li[1], Ke Jin[2], Gabi W. van Pelt[3], Hans van Dam[1], Xiao Yu[4], Wilma E. Mesker[3], Peter ten Dijke[1,2], Fangfang Zhou[1,5]*, Long Zhang[1,2]*

[1] Department of Molecular Cell Biology, Cancer Genomics Centre Netherlands and Centre for Biomedical Genetics, Leiden University Medical Center, Leiden, The Netherlands;
[2] Life Sciences Institute, Zhejiang University, Hangzhou, Zhejiang 310058, China; [3]Department of Surgery, [4]Department of Anatomy and Embryology, Leiden University Medical Center, Leiden, The Netherlands;
[5]Institutes of Biology and Medical Science, Soochow University, Suzhou 215123, PR China
*Address correspondence to:
Long Zhang, Life Sciences Institute, Zhejiang University, Hangzhou, Zhejiang 310058, China; Tel: +86-571-88208375; email: l_zhang@zju.edu.cn;

Fangfang Zhou, Institutes of Biology and Medical Science, Soochow University, Suzhou 215123, PR China. Tel: +86-512-65882491; email: zhoufangfang@suda.edu.cn;

Paper submitted

Abstract

The function and downstream pathways of transcription factor c-Myb in aggressive breast cancers are unclear. Here we demonstrate that c-Myb is required for pro-metastatic characters in basal breast cancer. Through analysis of breast cancer patients, we identified c-Myb as an activator of Wnt/β-catenin signaling. c-Myb could interact with the intracellular Wnt effector β-catenin and co-activates Wnt/β-catenin target genes Cyclin D1 and Axin2. Moreover, c-Myb controls breast cancer metastasis in an Axin2 dependent manner. Tissue microarray analysis of breast cancer patients indicated a positive association between c-Myb and Axin2. Furthermore, c-Myb is a target of the pro-inflammatory cytokine IL-1β and was found to be required for IL-1β-induced breast cancer cell invasion. Our results identify c-Myb as a promoter of breast cancer invasion and metastasis through activation of Wnt/β-catenin/Axin2 signaling.

Introduction

c-Myb was initially identified as a proto-oncogene associated with leukaemogenesis [1]. It encodes a transcription factor that regulates cell proliferation and differentiation in multiple cell types and is critical for normal haematopoiesis [2]. c-Myb can both activate and repress transcription and its target gene specificity is predominantly controlled by protein-protein interactions that occur outside its DNA binding domain [3]. Interestingly, increased expression of c-Myb is associated with malignant human cancers, such as colorectal cancer and adenoid cystic cancer [4, 5]. In addition, c-Myb overexpression, amplification and dysregulation has been detected in some subtypes of breast cancer [6]. In estrogen receptor positive (ER+) breast cancers, c-Myb expression is strongly induced by estrogen/ER signaling [7]. In ER+ cells, c-Myb is required for tumourigenesis and inhibits apoptosis in primary tumour cells; it is also involved in the TGF-β-induced epithelial-to-mesenchymal transition (EMT) process [8]. In addition, increasing evidence indicates that c-Myb is found in invasive breast cancer associated with poor prognosis [9]. However, the regulation of c-Myb activity and its downstream signaling networks in these processes remain largely unclear.

Wnt proteins are secreted cytokines that play pivotal roles during tumour initiation, progression and metastasis and modulate tumour cell survival, growth, migration and self-renewal [10]. In breast cancer, Wnt-induced signaling is a

promoter in EMT and invasion/metastasis [11], and components of the canonical Wnt signaling pathway have been identified as important mediators of breast cancer metastasis and as markers of poor prognosis [12]. The canonical Wnt/β-catenin signaling cascade is initiated when Wnt ligands interact with a heterodimeric transmembrane receptor complex, which consists of a seven-transmembrane domain protein with an N-terminal cysteine-rich domain named Frizzled (Fz) plus a low density lipoprotein receptor-related protein (LRP) [13]. In the absence of Wnt ligands, a 'destruction complex', consisting of Axin, casein kinase 1 (CK1), glycogen synthase kinase 3β (GSK3α/β) and adenomatous polyposis coli (APC), induces β-catenin phosphorylation and proteasomal degradation [14]. Upon Wnt binding the receptor complex, LRP is phosphorylated which triggers disruption of the β-catenin 'destruction complex'. This enables β-catenin to translocate to the nucleus and form a transcription activation complex with TCF/LEF (T-cell specific transcription factor/lymphoid enhancer-binding factor) that drives Wnt-induced gene expression [15] .

A number of Wnt target genes have been linked to oncogenesis, including *Cyclin D1* and *Axin2*. Activation of β-catenin correlates with strong expression of *Cyclin D1* in both breast cell lines and in patients, and this is associated with poor clinical outcome [16]. Axin2 is a Wnt suppressor and mediates negative feedback [17]. However, Axin2 also has tumour-promoting functions; it can for example trigger an EMT-like process in MCF7 and MDA-MB-231 breast cancer cells via stabilization of Snail [18]. In line with this, both the canonical Wnt pathway and Axin2 are activated in colorectal cancer, contributing to enhanced Snail expression, EMT and tumour invasion [19]. In the current study we demonstrate a mechanistic link between cMyb and Wnt/β-catenin signaling in basal breast cancer cells, which plays an important role in invasion and metastasis.

Materials and Methods

Cell culture and reagents

Human MDA-MB-231-luc (BM) cells were obtained as previous mentioned [20] and MDA-MB-231 cells were provided by ATCC. MDA-MB-231 and MDA-MB-435 cells are cultured in DMEM (high glucose with L-glutamine) supplemented with 10% FBS and 100 U/ml Pen/Strep (Gibco, Invitrogen). MCF10A-M2 cells were a kind gift from Dr. Fred Miller (Barbara Ann Karmanos Cancer Institute, Detroit, MI, USA). The cells were maintained in DMEM/F12 (Gibco) containing 5% horse serum (Gibco), 100 U/ml Pen/Strep

(Gibco), 0.5 µg/ml hydrocortisone (Sigma,), 10 µg/ml insulin (Sigma), 20 ng/ml epidermal growth factor (EGF) (Upstate) and 100 ng/ml cholera toxin (Calbiochem). All cell lines were maintained at 37°C with 5%CO_2.

Immunoblotting and immunoprecipitation

Cells were washed with PBS, scraped into iced tubes and lysed with TNE buffer (50 mM pH 7.4 Tris-HCl, 100 mM NaCl, 0.1 mM EDTA, 1% NP-40 and protease inhibitors) by incubation with agitation at 4°C for 5 min. Cells were spun down at 12,000 rpm at 4°C for 10 min to obtain supernatant. The protein concentration in the samples was measured using the DC protein assay (Bio-Rad), and the concentrations were adjusted to the same concentration for Western blotting. For immunoprecipitation, the supernatant was incubated with antibodies overnight or with anti-Flag M2 Affinity Gel (Sigma) for 2 hours at 4°C. After the precipitate was washed 3 times with TNE buffer, bound proteins were eluted with protein buffer at 100°C for 5 min. All Western blotting was performed with the Mini-Cell Electrophoresis System (Bio-Rad). We used the following primary antibodies: anti-N-cadherin (610920, BD Transduction Laboratories), anti-Slug (9585, Cell Signaling), anti-β-catenin (610154, BD Transduction Laboratories), anti-c-Myb (12319s, Cell Signaling), anti-LEF-1(2230, Cell Signaling), anti-Axin2 (2151 Cell Signaling), anti-tubulin (2148, Cell Signaling), anti-HA (1583816, Roche), anti-Flag (F3165, Sigma) and anti-β-actin (A5441, Sigma). All secondary antibodies were from Sigma.

Statistical analysis

The results are expressed as the mean ± s.d. (standard deviation). For analysis, we used Student's t-test, and $p<0.05$ was considered to be statistically significant. ∗: $0.01 < p < 0.05$, ∗∗: $0.0001 < p < 0.01$, ∗∗∗: $p < 0.0001$. The correlation between genes expression were analysed by Pearson's coefficient tests. For analysing TMA results. The χ^2 test was used to calculate correlation between c-Myb and Axin2.

Results

c-Myb is critical for pro-metastatic traits in breast cancer cells

To investigate the function of c-Myb in breast cancer progression, we first analysed copy number alterations of *c-Myb* in the TCGA Research Network (http://cancergenome.nih.gov) by cBioportal [21, 22]. *c-Myb* is amplified in

more than 2% of breast cancer patients, while 15% show *c-Myb* gain (Supplementary Fig. S1A). Notably, *c-Myb* amplification and gain is associated with a poor clinical outcome (Supplementary Fig. S1B). We then examined the expression level of *c-Myb* in breast cancer samples by analysing online clinical databases [22-25]. Oncomine plots show that *c-Myb* is highly expressed in both invasive ductal and lobular breast cancer, suggesting that c-Myb may play a role in tumour progression (Fig. 1A). Although the mRNA level of *c-Myb* is upregulated in most ER+ breast cancers, elevated *c-Myb* expression has also been observed in ER- breast cancers, which are frequently invasive and metastatic [26].

To study the function of c-Myb in breast cancer progression, we silenced endogenous c-Myb expression in two invasive basal breast cancer cell lines, MDA-MB-231 and MCF10A-M2, in which c-Myb protein was readily detected. Figure 1B showed the c-Myb knockdown efficiency in these cell lines at both mRNA and protein levels. Since breast cancer progression is associated with enhanced breast cancer migration and invasion [27], we first tested the effect of c-Myb knockdown on invasion/migration. In both MDA-MB-231 and MCF10A-M2 cells, depletion of c-Myb resulted in a significant decrease in cell invasiveness in a transwell assay (Fig. 1C). Since tumour progression and invasion is associated with an EMT phenotype, we next examined the effect of c-Myb depletion on various mesenchymal traits. In line with the putative tumour-promoting effect of c-Myb, we found that the mRNA levels of various mesenchymal markers, including *Twist*, *Snail* and *Slug*, were decreased in both MDA-MB-231 and MCF10A-M2 cells after c-Myb knockdown (Fig. 1D). In addition, immunoblotting showed decreased protein expression of N-cadherin, Slug and Snail in c-Myb-depleted cells (Fig. 1E). We also observed similar trends in MDA-MB-435 cells (Supplementary Fig. S2A and B). To investigate the relevance of our findings in terms of clinical data, we analysed the correlation of c-Myb and mesenchymal markers expression in a publicly available microarray database (GSE2990) [28]. Figure 1F showed that there was a positive correlation between the mRNA expression of *c-Myb* and mesenchymal makers like *N-Cadherin*, *Snail* and *Slug* in 189 breast cancer patients. We also examined the prognosis of the patients from this particular dataset and found that high expression of *c-Myb* is associated with a poorer clinical outcome (Fig. 1G). These clinical results are consistent with the experimental data indicating that c-Myb has a promoting role in breast cancer progression.

Figure1

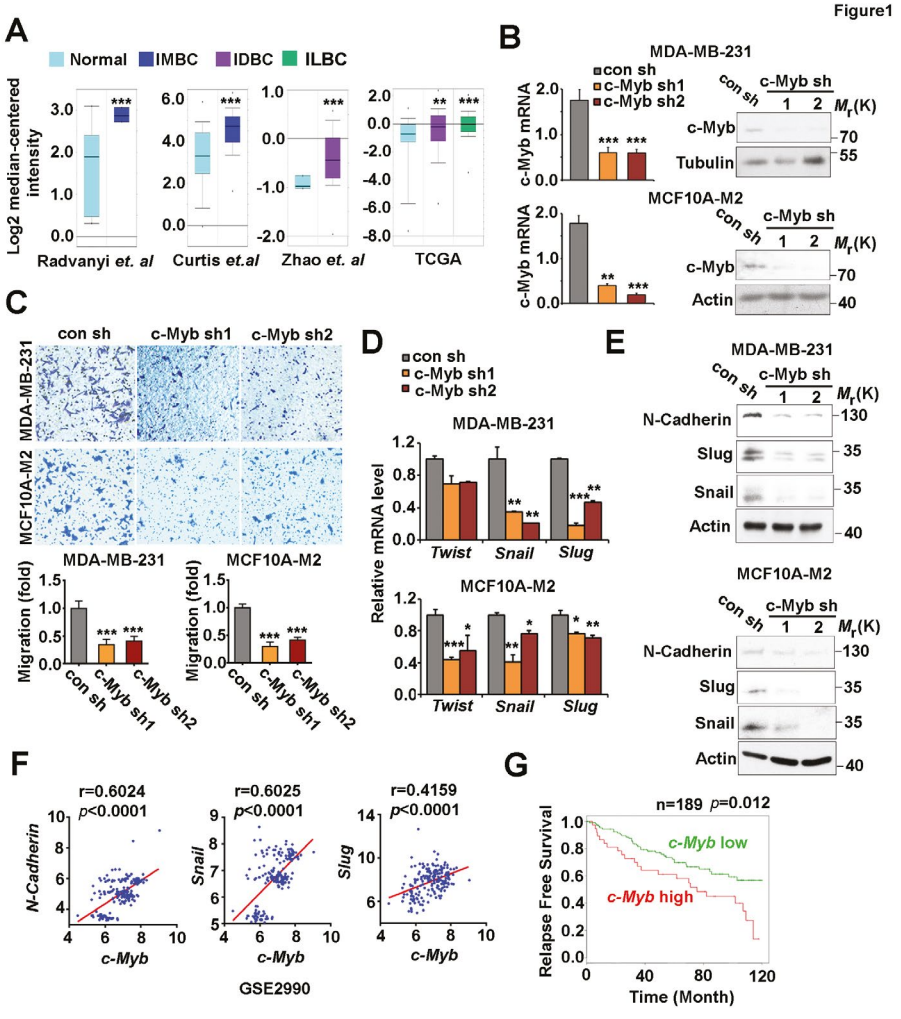

Figure 1. c-Myb is a potential activator of breast cancer invasion. A, Oncomine plots of c-Myb mRNA levels in normal breast tissue (normal), invasive mixed breast carcinoma (IMBC), invasive ductal breast carcinoma (IDBC), and invasive lobular breast carcinoma (ILBC) in public breast cancer datasets[22-25]. B, MDA-MB-231 cells and MCF10A-M2 cells stably expressing control shRNA (con sh) or two independent c-Myb shRNAs (sh1 and 2) were subjected to real-time quantitative PCR for c-Myb mRNA detection (left) or immunoblotting for c-Myb protein detection (right). mRNA levels of were normalized to *GAPDH* levels. Mean ± s.d. of triplicates, **p<0.01 ***p<0.001. Protein loading control was performed by immunoblotting for tubulin or actin. C, Transwell migration of control or c-Myb depleted MDA-MB-231 and MCF10A-M2 cells. Upper panel: representative images of migrated cells. Lower panel: fold changes of migrated cell numbers. D, qPCR analysis of mesenchymal markers in control or c-Myb depleted MDA-MB-231 (sh 1 and 2) and MCF10A-M2 (sh 1 and 2) cells. mRNA levels of the indicated genes were normalized to *GAPDH* levels. Mean ± s.d. of triplicates, *p<0.05 **p<0.01 ***p<0.001. E, Immunoblotting of mesenchymal markers in the indicated cells. Protein loading control was performed by immunoblotting for actin. F, Positive correlation between c-Myb mRNA and *N-Cadherin*, *Snail*, *Slug* mRNA expression in a clinical breast cancer dataset (GSE2990) [28]. Pearsons' coefficient tests were conducted to calculate statistical significance. G, Relapse free survival analysis of patients

with breast cancer with low or high *c-Myb* mRNA expression in the same breast cancer dataset.

c-Myb regulates breast tumour progression in zebrafish xenografts

We next tested the role of c-Myb on malignant breast cancer *in vivo* by using a zebrafish xenograft model. Red-fluorescence labelled breast cancer cells were transplanted into the duct of Cuvier (DoC) at 48 hours post fertilization (hpf) in Fli:GFP transgenic zebrafish [29]. The injected tumour cells can circulate in the blood vessels, extravasate from circulation and eventually metastasize into the tail fin of embryos after 6 days of implantation (Fig. 2A). When the zebrafish embryos were injected with the control MDA-MB-231 cells, 53% showed tumour cell progression into the tail fin; in contrast, embryos transplanted with c-Myb-depleted cells showed much less tumour progression (Fig. 2B and C). At all time points of the experiment, both the average invasive area and the percentages of embryos exhibiting metastasis were significantly lower in the two groups injected with c-Myb-depleted cells (Fig. 2D and E). In contrast to MDA-MB-231, MCF10A-M2 cells show moderate metastatic potential in this zebrafish model and form a cluster of cells in the caudal haematopoietic tissue (CHT) between the dorsal aorta and the caudal vein [30]. We therefore examined the effect of increased c-Myb levels by ectopic expression in MCF10A-M2 cells (Fig. 2F). The increased expression of c-Myb was found to enhance MCF10A-M2 cell migration *in vitro* (Supplementary Fig. S2C), which is in line with the pro-invasive function of c-Myb revealed by the knockdown results in Figure 1C. Forced c-Myb expression in MCF10A-M2 cells resulted in increased metastasis and a larger area of invasion in zebrafish embryo xenograft model (Fig. 2G-I). When the control MCF10A-M2 cells were implanted, 24% of the embryos showed tumour mass formation at 6 dpi. Ectopic expression of c-Myb in M2 cells increased this percentage nearly two-fold (45% of embryos), further confirming the positive role of c-Myb in breast cancer progression (Fig. 2J).

Figure2

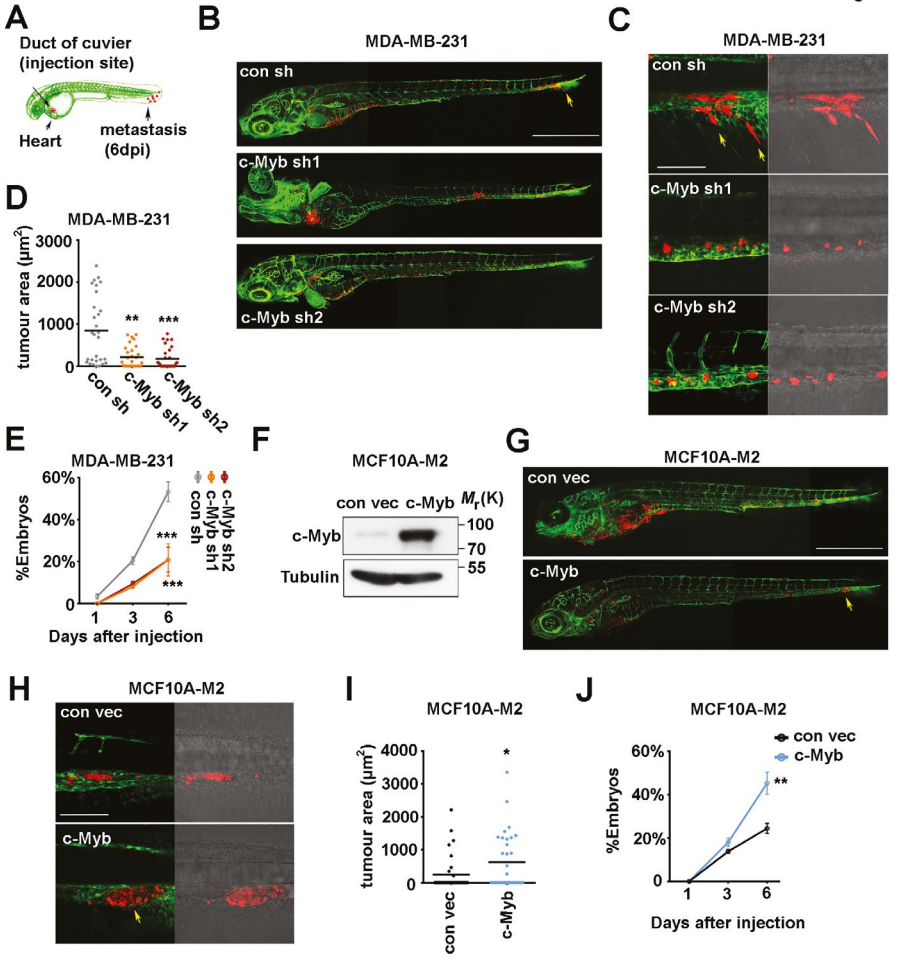

Figure 2. c-Myb positively controls breast cancer progression in a zebrafish model. A, Schematic representation of the zebrafish embryo xenograft assay. B, Control or c-Myb-depleted MDA-MB-231 cells stably expressing mCherry were injected into the duct of Cuvier (DoC) of Fli:GFP zebrafish embryos at 48 hpf. Overview image at 6 days post implantation (dpi). Arrows indicate metastatic tumour cells, scale bar: 500 µm. C, Detailed images of the tail fin. Arrows indicate metastatic tumour cells, scale bar: 100 µm. D, Area of metastatic cells in individual zebrafish embryos (n=29). $^{**}p<0.01$ $^{***}p<0.001$. E, Percentage of the zebrafish embryos displaying tumour progression to the tail fin. $^{***}p<0.001$. F, Immunoblotting of c-Myb in control or c-Myb overexpressing MCF10A-M2 cells. G, Overview image at 6 dpi of zebrafish embryos implanted with CM-DiI labeled control or c-Myb overexpressing MCF10-M2 cells. Arrows indicate metastatic tumour cells, scale bar: 500 µm. H, Detailed images of the tail fin. Arrows indicate metastatic tumour cells, scale bar: 100 µm. I, Area of metastatic cells in individual zebrafish embryos (n=33). $^{*}p<0.05$. J, Percentage of the zebrafish embryos displaying positive tumour progression to the tail fin. $^{**}p<0.01$.

c-Myb activates Wnt/β-catenin target genes and forms a complex with β-catenin/LEF-1 in breast cancer

Various signal transduction pathways have been found to induce and/or enhance tumour cell invasion and EMT [27]. We next investigated which signaling networks act at downstream of c-Myb to modulate breast cancer progression. For this we analysed the association between c-Myb and candidate signaling pathways, including the TGF-β, Wnt, NFκB and Notch pathways, using the TCGA Research Network (data not shown) [22] . We observed a significant positive correlation between c-Myb and three metastasis-associated direct targets of Wnt, namely *Axin2*, *LEF-1* and *Cyclin D1* among 534 breast cancer patients (Fig. 3A) [31]. In line with this, ectopic c-Myb expression in HEK293T cells consistently and significantly increased the transcriptional activity of the canonical Wnt reporter TOPFlash-Luc in a dose-dependent manner (Fig. 3B). Since previous studies showed that canonical Wnt signaling is required for migration, invasion and metastasis in breast cancer cell lines [18, 32], we subsequently investigated the possibility that c-Myb could function as an activator of the Wnt/β-catenin pathway during breast cancer progression. In line with this hypothesis the mRNA levels of the Wnt target genes *Axin2* and *Cyclin D1* were remarkably decreased in c-Myb deficient MDA-MB-231 and MCF10A-M2 cells upon stimulation with recombinant Wnt3a (100ng/ml) (Fig. 3C). These results suggested that c-Myb is required for the expression of Wnt target genes in these basal breast cancer cells.

The activation of transcription by canonical Wnt signaling is triggered by the binding of nuclear β-catenin to TCF/LEF transcription factors on target promoters. We previously reported that c-Myb can interact with LEF-1 in leukemic cells [33]. We therefore investigated the subcellular location and putative interaction between c-Myb and β-catenin. The Flag-tagged stable β-catenin mutant β-catenin SA and HA-tagged c-Myb indeed co-localized in the nucleus upon ectopic expression in HeLa and Cos-7 cells (Supplementary Fig. S3A). Moreover, the ectopically expressed HA-c-Myb was found to strongly interact with Flag-β-catenin in HEK293T cells (Fig. 3D). Co-immunoprecipitation experiments in MDA-MB-231, MCF10A-M2 and MDA-MB-435 cells also showed an interaction between endogenous c-Myb and β-catenin in basal breast cancer cells (Fig. 3E and Supplementary Fig. S3B). These findings suggested that c-Myb can activate canonical Wnt target genes by binding to β-catenin and/or LEF-1.

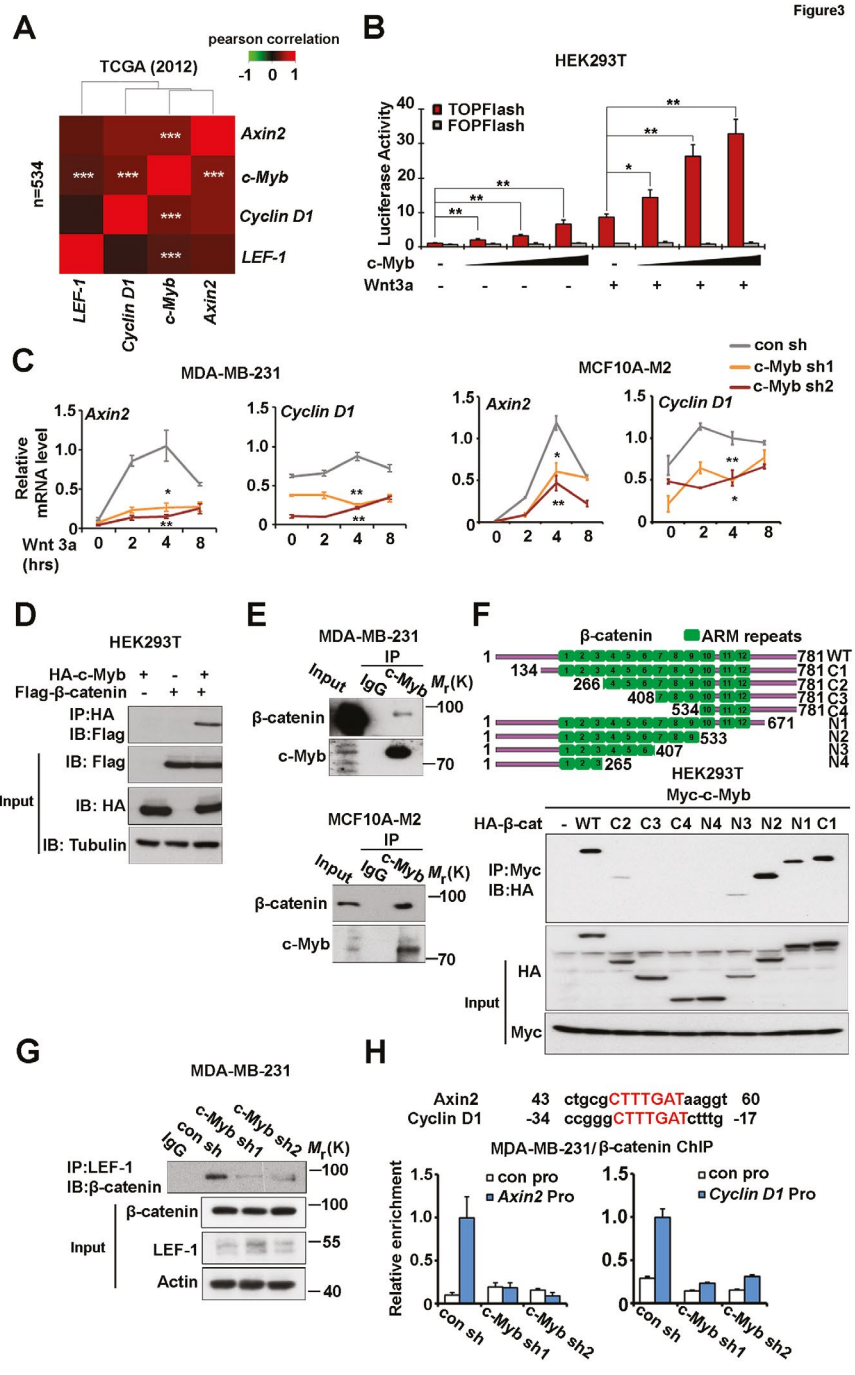
Figure3
A
pearson correlation
-1 0 1
TCGA (2012)
n=534
Axin2
c-Myb
Cyclin D1
LEF-1
B
HEK293T
TOPFlash
FOPFlash
Luciferase Activity
c-Myb
Wnt3a
C
MDA-MB-231
MCF10A-M2
con sh
c-Myb sh1
c-Myb sh2
Axin2
Cyclin D1
Relative mRNA level
Wnt 3a (hrs)
D
HEK293T
HA-c-Myb
Flag-β-catenin
IP:HA
IB:Flag
IB: Flag
IB: HA
IB: Tubulin
Input
E
MDA-MB-231
IP
Input
IgG
c-Myb
Mr(K)
β-catenin
c-Myb
MCF10A-M2
F
β-catenin
ARM repeats
WT
C1
C2
C3
C4
N1
N2
N3
N4
HEK293T
Myc-c-Myb
HA-β-cat
IP:Myc
IB:HA
HA
Myc
G
MDA-MB-231
IP:LEF-1
IB:β-catenin
β-catenin
LEF-1
Actin
H
Axin2 43 ctgcgCTTTGATaaggt 60
Cyclin D1 -34 ccgggCTTTGATctttg -17
MDA-MB-231/β-catenin ChIP
con pro
Axin2 Pro
Cyclin D1 Pro
Relative enrichment

Figure 3. c-Myb interacts with β-catenin and affects Wnt/β-catenin target gene expression**.** A, Correlation heatmap of c-Myb and Wnt target gene expression. Rows and columns are ranked by pearson correlation. Red: high correlation; green: low correlation. Branches represent relations between each gene profile of 534 breast patients in TCGA dataset [22]. *** $p<0.001$. B, Ectopic expression of c-Myb potentiates TOPFlash (but not FOPFlash) reporter activity in HEK293T cells with or without 100ng/ml recombinant Wnt3a treatment in a dose dependant manner. * $p<0.05$, ** $p<0.01$. C, Effect of c-Myb depletion on the expression of the Wnt target genes *Axin2* and *Cyclin D1* in MDA-MB-231 and MCF10A-M2 cells upon recombinant Wnt3 treatment (100ng/ml). mRNA levels of *Axin2* and *Cyclin D1* were analysed by qPCR and normalized to *GAPDH*; mean ± s.d. of triplicates. * $p<0.05$, ** $p<0.01$. D, Co-immunoprecipitation (Co-IP) of HA-c-Myb and Flag-β-catenin transfected in HEK293T cells as indicated (IP: immunoprecipitation; IB: immunoblot). Tubulin IB was performed to control for protein loading. E, Endogenous interaction between c-Myb and β-catenin detected by immunoblotting of Co-IP samples from MDA-MB-231 and MCF10-M2 cells. F, Upper panel: schematic representation of HA-β-catenin deletion mutants tested. Lower panel: Co-IP of Myc-c-Myb and HA-β-catenin deletion mutants transfected in HEK293T cells and detected by immunoblotting. Input samples were blotted with HA and Myc antibody. G, Endogenous interaction between LEF-1 and β-catenin in control and c-Myb knockdown MDA-MB-231 cells detected by immunoblotting of Co-IP samples. H, Chromatin immunoprecipitation (ChIP) of β-catenin in control and c-Myb depleted MDA-MB-231 cells. Upper panel: Sequence and location of the analysed TCF binding motifs in the *Axin2* (48 from transcription start site) and *Cyclin D1* (-23 from transcription start site) genes. Lower panel: chromatin-bound β-catenin detected by qRT-PCR. The Actin promoter served as control promoter (con pro). Input genomic DNA was used for normalization, mean ± s.d. of triplicates.

Subsequent analysis of the binding of c-Myb to progressive deletion mutants of β-catenin showed that the amino-terminal activating arm (NTAA) of the armadillo repeat (ARM) domain of β-catenin (3-6 repeats) is essential for the interaction (Fig. 3F). This ARM motif is important for the binding of β-catenin co-factors involved in transcriptional activation of Wnt target genes, and in addition for TCF/LEF binding (4–10 repeats) [34]. Importantly, we found that the interaction between β-catenin and LEF-1 was reduced when c-Myb was knocked down in MDA-MB-231 cells (Fig. 3G). Moreover, chromatin immunoprecipitations showed that depletion of c-Myb inhibited the recruitment of β-catenin to the promoters of *Axin2* and *Cyclin D1* (Fig. 3H). Taken together, these data suggest that c-Myb acts as a β-catenin co-factor that stabilizes its interaction with TCF/LEF and thereby can enhance Wnt signaling-induced transcription.

c-Myb promotes breast tumour progression through Axin2

As a direct target gene of Wnt/β-catenin, Axin2 not only mediates negative feedback [17], but also can enhance EMT and cancer progression [18]. In line with the RNA data in Figure 3, the Axin2 protein level was strongly decreased in c-Myb-depleted MDA-MB-231 cells (Fig. 4A). We therefore examined the role of Axin2 in c-Myb-induced breast cancer invasion/metastasis. For this, we depleted Axin2 in both normal MDA-MB-231 cells and MDA-MB-231

Figure 4

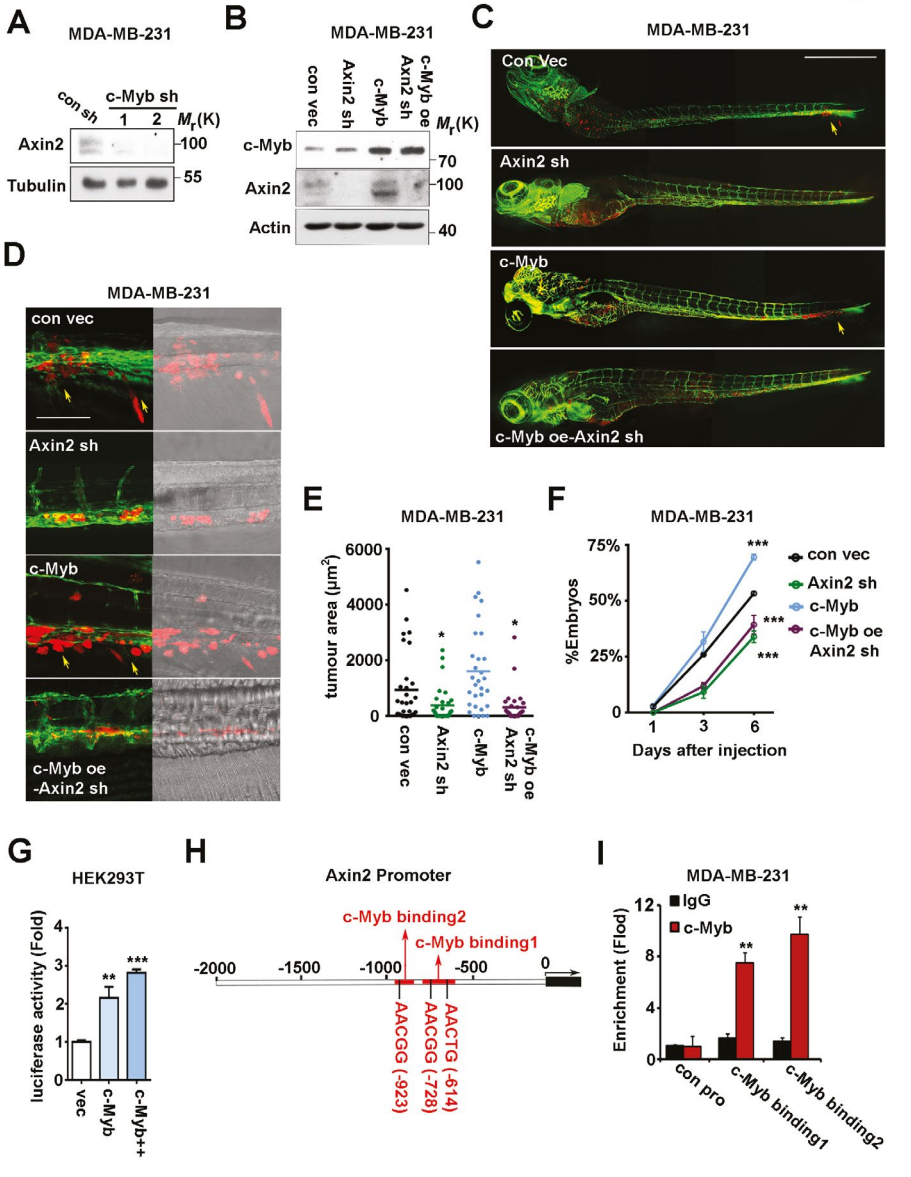

Figure 4.c-Myb-induced breast cancer metastasis in zebrafish mediated via Axin2 induction. A, Axin2 protein levels in control and c-Myb depleted MDA-MB-231 cells as detected by immunoblotting. Tubulin immunoblot was performed to control for protein loading. B, Immunoblot detection of the c-Myb and Axin2 protein levels in MDA-MB-231 cells infected with lentivirus-control vector (con vec) , Axin2 shRNA vector, c-Myb overexpression vector or both Axin2 shRNA and c-Myb overexpression vectorsas indicated. C, Representative overview images at 6 days post implantation (dpi) of zebrafish injected with MDA-MB-231 cells shown under B labeled with mCherry. Arrows indicate metastatic tumour cells, scale bar: 500 μm. D, Detailed images of the tail fin. Arrows indicate metastatic tumour cells, scale bar: 100 μm. E, Area of metastatic cells in individual

zebrafish embryos (n = 30). *p<0.05. F, Percentage of the zebrafish embryos displaying tumour progression to the tail fin ***p<0.001. G, Ectopic expression of c-Myb induces an *Axin2* promoter-driven luciferase reporter in HEK293T cells [17]. **p<0.01 ***p<0.001. H, Schematic diagram of the *Axin2* promoter showing three c-Myb binding sites and the 2 binding regions (red) analysed by chromatin immunoprecipitation in (I). I, Chromatin IP (ChIP) of *Axin2* promoter-bound c-Myb in MDA-MB-231 cells. qPCR was performed with primers for the 2 c-Myb binding regions shown in (G). The *Actin* promoter served as control promoter (con pro). Input genomic DNA was used for normalization, mean ± s.d. of triplicates. **p<0.01

cells ectopically overexpressing c-Myb, in which the endogenous Axin2 protein levels are increased by c-Myb (Fig. 4B). Figure 4B also shows that Axin2 expression was efficiently blocked by Axin2-specific shRNA. These MDA-MB-231 cells were subsequently injected into the duct of Cuvier of zebrafish to analyse their metastatic potential (Fig. 4C and D). Compared to the embryos injected with the control cells, the embryos implanted with c-Myb-overexpressing cells showed a higher tumour area and an increased percentage of tumour progression to the tail fin (70% vs. 53% in controls) (Fig. 4E and F). Moreover, the depletion of Axin2 significantly repressed invasion and metastasis in both the control MDA cells and the c-Myb overexpressing cells (Fig. 4E and F). Thus, the c-Myb-induced zebrafish metastasis of these basal breast cancer cells is dependent on Axin2.

Because *Axin2* turned out to be a critical target gene of c-Myb in breast cancer cell invasion, we further analysed the mechanism by which c-Myb activates *Axin2* gene expression. Since c-Myb is a sequence specific DNA binding protein, we examined whether it can bind and regulate the *Axin2* promoter directly. Ectopic expression of c-Myb could significantly induce *Axin2* promoter-driven luciferase reporter in HEK293T cells (Fig. 4G).We identified three potential c-Myb binding motifs (TAACt/gG) [35] in the *Axin2* promoter at positions -923, -728 and -614. Next, we performed chromatin immunoprecipitations to specifically analyse the binding of c-Myb to the region encompassing, the two proximal c-Myb binding sites (c-Myb binding 1, -745 to -598), and the region encompassing the more distal site (c-Myb binding 2 ,-959 to -858) (Fig. 4H). Enrichment for c-Myb was detected at both c-Myb binding regions in MDA-MB-231 cells (Fig. 4I). Together, these results indicate that c-Myb can directly bind to the *Axin2* promoter to stimulate *Axin2* expression and induce an invasive phenotype in MDA- MB- 231 cells.

Loss of c-Myb suppresses breast cancer bone metastasis

We next examined the role of c-Myb in bone metastasis of MDA-MB-231

Figure 5

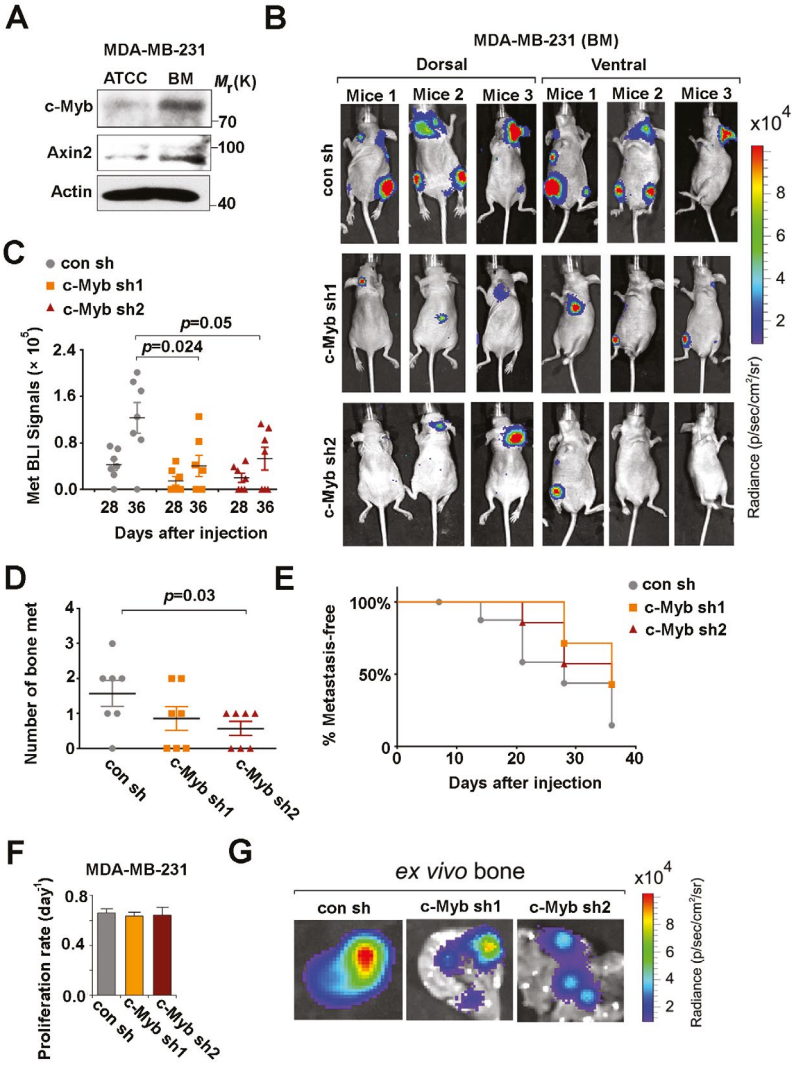

Figure 5. c-Myb knockdown in MDA-MB-231 BM cells impairs bone metastasis in mice**.** A, c-Myb and Axin2 protein in MDA-MB-231 cells from ATCC and the BM subline detected by immunoblotting. Actin immunoblot was performed to control for protein loading. B, Representative bioluminescent (BLI) images of mice injected intracardially with control or c-Myb depleted MDA-MB-231 BM cells at 36 days after injection. C, Normalized BLI signals in mice injected with control or c-Myb depleted MDA-MB-231 BM cells at 28 and 36 days after injection. D, Number of bone metastasis nodules at 36 days after injection. E, Percentage of bone metastasis-free mice. F, Cell proliferation rates *in vitro* of control and c-Myb depleted MDA-MB-231 BM cells. G, Representative BLI signals of bone metastasis *ex vivo.*

cells after intracardial injection in mice. First, we analysed the expression of c-Myb and Axin2 in parental MDA-MB-231 cells (ATCC) and its derivative bone metastatic line (BM), a highly metastatic subclone of MDA-MB-231 that displays a unique preference for dissemination to bone [20]. This experiment showed that both c-Myb and Axin2 are up-regulated in the highly metastatic MDA-MB-231 BM cells (Fig. 5A). We subsequently performed xenograft experiments in a mouse model for breast cancer metastasis [36]. Mice that were injected intracardially with control MDA-MB-231 BM cells began to develop detectable bone metastasis after 3 weeks, and the following 2 weeks (i.e. the last 2 weeks of the 5-week experimental period) were marked by expansion of the metastatic area. In contrast, mice injected with c-Myb-depleted BM cells developed less bone metastases after 36 days (Fig. 5B). Both of BLI signal and number of metastatic nodules was significantly decreased in the c-Myb-depleted groups (Fig. 5C and D). The mice implanted with c-Myb- deficient cells also displayed delayed appearance of metastatic signals (Fig. 5E). Importantly, the c-Myb-depleted cells did not show significant proliferation defects (Fig. 5F). To confirm the results of the live imaging experiments shown in Figure 5B-E, we euthanized the mice and observed lower bioluminescence signals in c-Myb-depleted groups in isolated metastatic nodules (Fig. 5G). Together, these data show that c-Myb also contributes to breast cancer metastasis in a mouse model.

High c-Myb expression shows a positive correlation with Axin2 expression in clinical cases

To determine the clinical relevance of the relation between c-Myb and Axin2 shown above, we performed immunohistochemistry (IHC) staining of tissue microarrays (TMAs) that included 176 breast cancer samples collected at Leiden University Medical Centre (Supplementary Table S1). Nuclear expression of c-Myb and cytoplasmic expression of Axin2 were subjectively scored as high staining or low staining (Fig. 6A). Based on the role of c-Myb in promoting tumour invasion and metastasis, we first examined the relation between c-Myb and regional lymph node invasion. As Figure 6B shows, c-Myb up-regulation positively associated with lymph node invasion. Next, we investigated the correlation between c-Myb and Axin2 in the same tissue microarray. Consistent with the result that c-Myb activates Axin2 in breast cancer, we observed that more than 70% of Axin2 high expression samples also have high c-Myb expression (Fig. 6C). *Vice versa* the c-Myb levels were significantly positively correlated with Axin2 expression (Fig. 6D). These data support our findings that c-Myb enhances Axin2 expression and that this induces an aggressive phenotype and poor prognosis in human breast cancer.

Figure 6

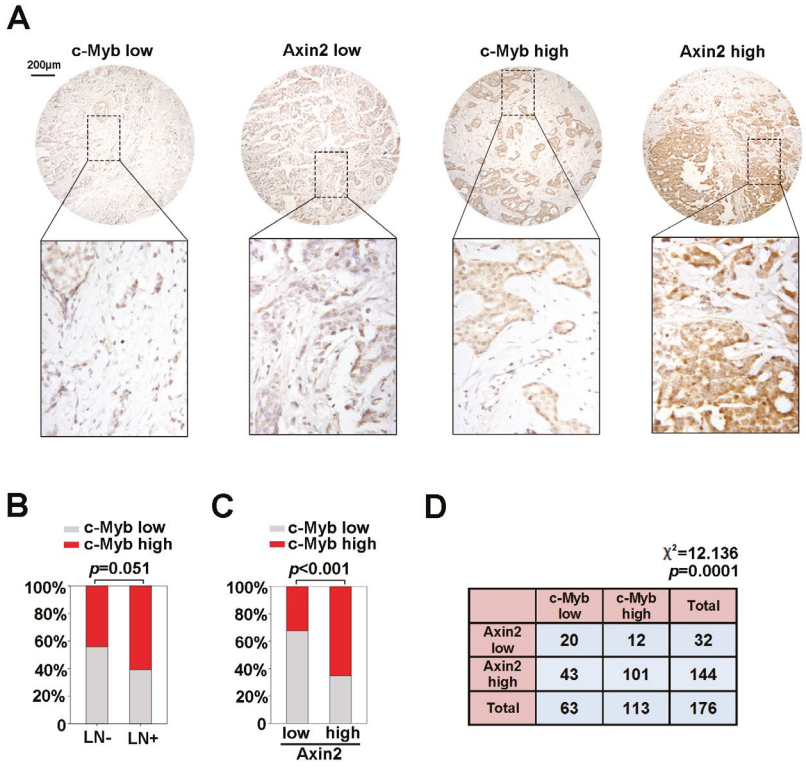

	c-Myb low	c-Myb high	Total
Axin2 low	20	12	32
Axin2 high	43	101	144
Total	63	113	176

Figure 6. c-Myb correlates with Axin2 in breast cancer patients. A, Representative images of c-Myb and Axin2 immunohistochemistry of breast cancer tissue. Upper panel: objective: 5×, scale bar: 200μm. Lower panel: objective: 25×. B, Percentage of patient samples with high or low c-Myb expression showing in negative (LN-) or positive (LN+) lymph node invasion. C, Percentage of samples with low or high c-Myb expression in relation to the expression levels of Axin2. D, Correlation analysis of c-Myb and Axin2 expression in the same tissue microarray. χ^2 = 12.136, p = 0.0001.

Interleukin-1β (IL-1β) stimulates c-Myb expression in ER- breast cancer

To search for mechanisms that contribute to c-Myb expression in breast cancer, we tested several cytokines to see if they regulated c-Myb expression in the ER- MDA-MB-231 breast cancer cell line. The inflammatory cytokine IL-1β was found to increase c-Myb mRNA levels (Fig. 7A). Similarly, the

Figure 7

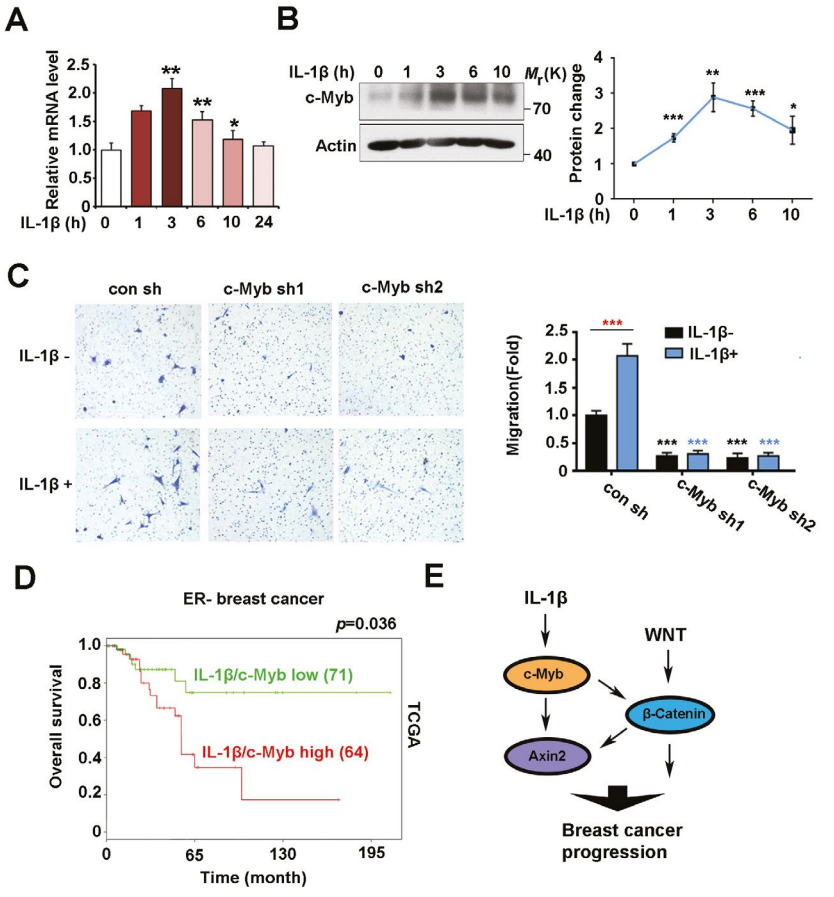

Figure 7. c-Myb is regulated by IL-1β. A, qPCR analysis of c-Myb mRNA levels in MDA-MB-231 cells treated with 10 ng/ml IL-1β for the indicated times. **p*<0.05, ***p*<0.01. B, Left, immunoblotting of c-Myb protein in MDA-MB-231 cells treated with IL-1β for the indicated times. Right, quantification of the protein levels. Mean ± s.d. , **p*<0.05 ***p*<0.01 ****p*<0.001. C, Transwell migration of control or c-Myb depleted MDA-MB-231 cells treated with or without 10ng/ml IL-1β for 16 h. Left, representative images of migrated cells. Right, fold changes of migrated cell numbers, mean ± s.d.. D, Overall survival analysis of patients in breast cancer with both low *c-Myb* and *IL-1β* or both high *c-Myb* and *IL-1β* mRNA expression in TCGA ER- breast cancer dataset by PROGgene.

E, Proposed model of the role of c-Myb in breast cancer.

c-Myb protein level increased significantly from 1h to 10 h after 10 ng/ml IL-1β treatment, peaking at 3 hours (Fig. 7B). Members of the IL-1 family of cytokines are abundantly expressed in the microenvironment of breast cancer and are indispensable for tumour progression [37]. To test whether c-Myb is functionally involved in the IL-1β response, we examined the effect of c-Myb depletion on IL-1β-stimulated cell migration. Interestingly, both basal and IL-

1β-induced MDA-MB-231 cell migration was effectively blocked by c-Myb knockdown (Fig. 7C), indicating that c-Myb is essential for IL-1β-mediated tumour cell migration. This prompted us to re-analyse the TCGA dataset by PROGgene [22, 38]. For the ER- breast cancer patients, high expression of both IL-1β and c-Myb was significantly associated with poor prognosis (Fig. 7D). Collectively, these results indicate that IL-1β is associated with c-Myb activation and leads to poor survival in ER- breast cancer.

Discussion

Our study suggests a model in which c-Myb is activated by IL-1β and interacts with β-catenin in the nuclear. c-Myb then acts as a co-factor of β-catenin and accelerates expression of genes that are downstream of β-catenin in breast cancer. In addition, c-Myb also directly binds to the Axin2 promoter and drives Axin2 expression enhancing breast tumour progression (Fig. 7E).

Transcription factor c-Myb previously has been found to play a functional role in ER positive breast cancer by enhancing proliferation and inhibiting differentiation c-Myb expression can be induced by ER and high c-Myb predicts good survival in ER+ breast cancers that can be efficiently treated [7, 9]. The role of Myb in EMT, invasion and metastasis is less clear, and is likely to depend on the exact genetic changes and pathway defects in the tumour and on the tumour microenvironment Transcriptional events mediated by estrogen signaling have a distinct role in development and proliferation in the early stages of a tumour, and the ER target GATA3 and can negatively regulate metastasis [39], whereas FOXA1 positively correlates with distant metastasis[40]. Moreover, c-Myb can regulate tumour migration *in vitro* in both ER+ and ER- cell lines [8, 41]. In this study, we found that c-Myb is specifically required for breast cancer invasion and metastasis in experimental xenograft models in zebrafish and mice. As one of the signature proteins that correlates with ER status, c-Myb has also been implicated in survival in luminal/ER+ breast cancer and is linked to the regulation of BCL2 [22, 42]. However, we observed no significant proliferation or survival defects after knockdown of c-Myb in ER- cell lines.

One of the signaling pathways involved in breast cancer progression is the Wnt pathway, which can induce both EMT and invasion/metastasis [11, 43]. Importantly, we found c-Myb to enhance the expression levels of various target genes of Wnt /β-catenin signaling, including cyclin D1 and Axin2, by functionally interacting with LEF-1/β-catenin and facilitating β-catenin binding to its target promoters. In addition, c-Myb was found to bind to the

Axin2 promoter directly, and thereby to induce Axin2 expression and enhance breast tumour progression. We further show that c-Myb expression in breast cancer cells can be activated by IL-1β , which suggests that c-Myb may in particular enhance migration and invasion in response to inflammatory signals in the tumour microenvironment. In this respect it is interesting to note that c-Myb can contribute to TGF-β-induced epithelial-to-mesenchymal transition (EMT) in ER+ breast cancer cells [8]. It might therefore be interesting to investigate the IL-1β/TGF-β/Wnt interplay in this process.

The exact mechanism by which c-Myb enhances Wnt/β-catenin inducible genes remains to be established. β-catenin can interact with both LEF1/TCF and Wnt co-activators/repressors through its ARM domain which consists of 12 repeats [44]. Our results demonstrated that c-Myb binds to the NTAA motif of the ARM domain. β-catenin co-factors like Pontin and Reptin both have been reported to bind to the NTAA motif of β-catenin and act as antagonistic modifiers of Wnt–induced target genes [45]. Consistent with this model, we observed decreased expression of Wnt target genes and reduced binding affinity of β-catenin to the corresponding promoters when c-Myb was knocked down in MDA-MB-231 cells. These data indicates c-Myb might therefore act as a β-catenin co-activator in breast cancer.

Our results further suggest that c-Myb positively controls various mesenchymal markers to contribute to local invasion and distant metastasis of cancer, since mesenchymal signatures like Twist, Snail, Slug and N-cadherin are significantly decreased in c-Myb-deficient breast cell lines. Moreover, Wnt signaling can promote EMT by inducing the expression of the these mesenchymal markers during breast cancer invasion [12, 46], further supporting our observation that Wnt-β-catenin signaling might contribute to c-Myb-induced cancer progression. In this context, we also found that c-Myb is highly expressed in tumours with lymph node invasion in breast cancer patients, suggesting that c-Myb is required for the pro-metastatic phenotype.

Depletion of c-Myb was found to impair breast cancer bone metastasis in a mouse model. Therefore, c-Myb appears to be required for the spreading of advanced metastatic cells to bone. We found that two direct target genes of Wnt signaling, Cyclin D1 and Axin2, were decreased by c-Myb depletion. Both genes are likely to contribute to c-Myb-induced tumour progression. Although Cyclin D1 facilitates cell cycle progression, there is no correlation between cell proliferation and Cyclin D1 expression in samples from breast cancer patients [47], but high expression of Cyclin D1 promotes local invasion and is associated with bone metastasis [48]. Axin2 can fine-tune Wnt signaling and counteract excessive signaling as a Wnt feedback inhibitor, but,

more importantly, Axin2 also acts as a chaperone for GSK3β and controls its subcellular location in human breast cancer. As a result of this Snail is dephosphorylated and stabilized, contributing to EMT and invasion [18]. Moreover, we previously demonstrated that Axin2 can form a complex with the E3 ligases Rnf12 and Arkadia and induce Smad7 degradation to promote TGF-β signaling and breast bone metastasis [49]. Importantly, we found a positive correlation between c-Myb and Axin2 in clinical samples.

Long-term clinical observations and mechanistic studies have shown a strong association of inflammation with cancer development and progression. Inflammation can result in an influx of inflammatory cells and secretion of inflammatory cytokines including TNFα, IL-1, IL-6 and IL-8 into the tumour microenvironment, leading to activation of the NF-κB pathway [50]. We not only found that IL-1β effectively induces c-Myb but also showed that c-Myb has a positive role in IL-1β-induced tumour migration. Clinically, high c-Myb and IL-1β expression was found to be linked with poor survival in ER- breast cancer. Therefore, our results suggest that levels of c-Myb and IL-1β might be important to predict the aggressiveness of specific breast cancers.

Author's contributions

Y.L. designed, performed experiments, analyzed and interpreted the results and wrote the manuscript; F. Z and L.Z. designed, performed experiments and wrote the manuscript; K. J performed mouse metastasis experiments. G.W.P, and W. E. M performed pathology analysis of the specimens. X. Y performed online clinical data analysis. H.v. D involved in the discussion and writing. P.t.D. directed the research, interpreted the data and wrote the manuscript.

Acknowledgments

We thank Dr. Odd Stokke Gabrielsen gifts the HA-c-Myb plasmid, Dr. Frank Costantini provided Axin2 reporter constructs. Dr. Zhijie Chang gifts the TOPFlash reporter. We thank all members of PtD lab for discussion.

Grant Support

This work is supported by the Cancer Genomics Centre Netherlands, Swedish Cancerfonden (09 0773), Zhejiang Provincial Natural Science Foundation of China (grant number R14C070002), The Chinese National Natural Science Funds (grant number 31471315) and the Netherlands Organization for Health

Research and Development (ZonMW grant number 8238-20864).

References

1. Klempnauer KH, Gonda TJ, Bishop JM: **Nucleotide sequence of the retroviral leukemia gene v-myb and its cellular progenitor c-myb: the architecture of a transduced oncogene**. *Cell* 1982, **31**(2 Pt 1):453-463.
2. Gewirtz AM, Calabretta B: **A c-myb antisense oligodeoxynucleotide inhibits normal human hematopoiesis in vitro**. *Science* 1988, **242**(4883):1303-1306.
3. George OL, Ness SA: **Situational awareness: regulation of the myb transcription factor in differentiation, the cell cycle and oncogenesis**. *Cancers* 2014, **6**(4):2049-2071.
4. Biroccio A, Benassi B, D'Agnano I, D'Angelo C, Buglioni S, Mottolese M, Ricciotti A, Citro G, Cosimelli M, Ramsay RG *et al*: **c-Myb and Bcl-x overexpression predicts poor prognosis in colorectal cancer: clinical and experimental findings**. *The American journal of pathology* 2001, **158**(4):1289-1299.
5. West RB, Kong C, Clarke N, Gilks T, Lipsick JS, Cao H, Kwok S, Montgomery KD, Varma S, Le QT: **MYB expression and translocation in adenoid cystic carcinomas and other salivary gland tumors with clinicopathologic correlation**. *The American journal of surgical pathology* 2011, **35**(1):92-99.
6. Kauraniemi P, Hedenfalk I, Persson K, Duggan DJ, Tanner M, Johannsson O, Olsson H, Trent JM, Isola J, Borg A: **MYB oncogene amplification in hereditary BRCA1 breast cancer**. *Cancer research* 2000, **60**(19):5323-5328.
7. Drabsch Y, Hugo H, Zhang R, Dowhan DH, Miao YR, Gewirtz AM, Barry SC, Ramsay RG, Gonda TJ: **Mechanism of and requirement for estrogen-regulated MYB expression in estrogen-receptor-positive breast cancer cells**. *Proceedings of the National Academy of Sciences of the United States of America* 2007, **104**(34):13762-13767.
8. Cesi V, Casciati A, Sesti F, Tanno B, Calabretta B, Raschella G: **TGFbeta-induced c-Myb affects the expression of EMT-associated genes and promotes invasion of ER+ breast cancer cells**. *Cell cycle* 2011, **10**(23):4149-4161.
9. Ramsay R: **Myb: getting involved in EMT**. *Cell cycle* 2012, **11**(3):433-434.
10. Anastas JN, Moon RT: **WNT signalling pathways as therapeutic targets in cancer**. *Nat Rev Cancer* 2013, **13**(1):11-26.
11. Dey N, Barwick BG, Moreno CS, Ordanic-Kodani M, Chen Z, Oprea-Ilies G, Tang W, Catzavelos C, Kerstann KF, Sledge GW, Jr. *et al*: **Wnt signaling in triple negative breast cancer is associated with metastasis**. *BMC cancer* 2013, **13**(1):537.
12. DiMeo TA, Anderson K, Phadke P, Fan C, Perou CM, Naber S, Kuperwasser C: **A novel lung metastasis signature links Wnt signaling with cancer cell self-renewal and epithelial-mesenchymal transition in basal-like breast cancer**. *Cancer research* 2009, **69**(13):5364-5373.
13. Janda CY, Waghray D, Levin AM, Thomas C, Garcia KC: **Structural basis of Wnt recognition by Frizzled**. *Science* 2012, **337**(6090):59-64.
14. Nelson WJ, Nusse R: **Convergence of Wnt, beta-catenin, and cadherin path-**

ways. *Science* 2004, **303**(5663):1483-1487.
15. Clevers H, Nusse R: **Wnt/beta-catenin signaling and disease**. *Cell* 2012, **149**(6):1192-1205.
16. Lin SY, Xia W, Wang JC, Kwong KY, Spohn B, Wen Y, Pestell RG, Hung MC: **Beta-catenin, a novel prognostic marker for breast cancer: its roles in cyclin D1 expression and cancer progression**. *Proceedings of the National Academy of Sciences of the United States of America* 2000, **97**(8):4262-4266.
17. Jho EH, Zhang T, Domon C, Joo CK, Freund JN, Costantini F: **Wnt/beta-catenin/Tcf signaling induces the transcription of Axin2, a negative regulator of the signaling pathway**. *Molecular and cellular biology* 2002, **22**(4):1172-1183.
18. Yook JI, Li XY, Ota I, Hu C, Kim HS, Kim NH, Cha SY, Ryu JK, Choi YJ, Kim J *et al*: **A Wnt-Axin2-GSK3beta cascade regulates Snail1 activity in breast cancer cells**. *Nature cell biology* 2006, **8**(12):1398-1406.
19. Wu ZQ, Brabletz T, Fearon E, Willis AL, Hu CY, Li XY, Weiss SJ: **Canonical Wnt suppressor, Axin2, promotes colon carcinoma oncogenic activity**. *Proceedings of the National Academy of Sciences of the United States of America* 2012, **109**(28):11312-11317.
20. Deckers M, van Dinther M, Buijs J, Que I, Lowik C, van der Pluijm G, ten Dijke P: **The tumor suppressor Smad4 is required for transforming growth factor beta-induced epithelial to mesenchymal transition and bone metastasis of breast cancer cells**. *Cancer research* 2006, **66**(4):2202-2209.
21. Gao J, Aksoy BA, Dogrusoz U, Dresdner G, Gross B, Sumer SO, Sun Y, Jacobsen A, Sinha R, Larsson E *et al*: **Integrative analysis of complex cancer genomics and clinical profiles using the cBioPortal**. *Science signaling* 2013, **6**(269):pl1.
22. Cancer Genome Atlas N: **Comprehensive molecular portraits of human breast tumours**. *Nature* 2012, **490**(7418):61-70.
23. Curtis C, Shah SP, Chin SF, Turashvili G, Rueda OM, Dunning MJ, Speed D, Lynch AG, Samarajiwa S, Yuan Y *et al*: **The genomic and transcriptomic architecture of 2,000 breast tumours reveals novel subgroups**. *Nature* 2012, **486**(7403):346-352.
24. Radvanyi L, Singh-Sandhu D, Gallichan S, Lovitt C, Pedyczak A, Mallo G, Gish K, Kwok K, Hanna W, Zubovits J *et al*: **The gene associated with trichorhinophalangeal syndrome in humans is overexpressed in breast cancer**. *Proceedings of the National Academy of Sciences of the United States of America* 2005, **102**(31):11005-11010.
25. Zhao H, Langerod A, Ji Y, Nowels KW, Nesland JM, Tibshirani R, Bukholm IK, Karesen R, Botstein D, Borresen-Dale AL *et al*: **Different gene expression patterns in invasive lobular and ductal carcinomas of the breast**. *Molecular biology of the cell* 2004, **15**(6):2523-2536.
26. Gonda TJ, Leo P, Ramsay RG: **Estrogen and MYB in breast cancer: potential for new therapies**. *Expert opinion on biological therapy* 2008, **8**(6):713-717.
27. Yilmaz M, Christofori G: **EMT, the cytoskeleton, and cancer cell invasion**. *Cancer metastasis reviews* 2009, **28**(1-2):15-33.
28. Sotiriou C, Wirapati P, Loi S, Harris A, Fox S, Smeds J, Nordgren H, Farmer P, Praz V, Haibe-Kains B *et al*: **Gene expression profiling in breast cancer: un-**

derstanding the molecular basis of histologic grade to improve prognosis. *Journal of the National Cancer Institute* 2006, **98**(4):262-272.

29. Li Y, Drabsch Y, Pujuguet P, Ren J, van Laar T, Zhang L, van Dam H, Clement-Lacroix P, Ten Dijke P: **Genetic depletion and pharmacological targeting of alphav integrin in breast cancer cells impairs metastasis in zebrafish and mouse xenograft models**. *Breast cancer research : BCR* 2015, **17**(1):28.
30. Drabsch Y, He S, Zhang L, Snaar-Jagalska BE, ten Dijke P: **Transforming growth factor-beta signalling controls human breast cancer metastasis in a zebrafish xenograft model**. *Breast cancer research : BCR* 2013, **15**(6):R106.
31. Nguyen DX, Chiang AC, Zhang XH, Kim JY, Kris MG, Ladanyi M, Gerald WL, Massague J: **WNT/TCF signaling through LEF1 and HOXB9 mediates lung adenocarcinoma metastasis**. *Cell* 2009, **138**(1):51-62.
32. Wu ZQ, Li XY, Hu CY, Ford M, Kleer CG, Weiss SJ: **Canonical Wnt signaling regulates Slug activity and links epithelial-mesenchymal transition with epigenetic Breast Cancer 1, Early Onset (BRCA1) repression**. *Proceedings of the National Academy of Sciences of the United States of America* 2012, **109**(41):16654-16659.
33. Zhou F, Zhang L, van Laar T, van Dam H, Ten Dijke P: **GSK3beta inactivation induces apoptosis of leukemia cells by repressing the function of c-Myb**. *Molecular biology of the cell* 2011, **22**(18):3533-3540.
34. Stadeli R, Hoffmans R, Basler K: **Transcription under the control of nuclear Arm/beta-catenin**. *Current biology : CB* 2006, **16**(10):R378-385.
35. Andersson KB, Berge T, Matre V, Gabrielsen OS: **Sequence selectivity of c-Myb in vivo. Resolution of a DNA target specificity paradox**. *The Journal of biological chemistry* 1999, **274**(31):21986-21994.
36. Kang Y, Siegel PM, Shu W, Drobnjak M, Kakonen SM, Cordon-Cardo C, Guise TA, Massague J: **A multigenic program mediating breast cancer metastasis to bone**. *Cancer cell* 2003, **3**(6):537-549.
37. Pantschenko AG, Pushkar I, Anderson KH, Wang Y, Miller LJ, Kurtzman SH, Barrows G, Kreutzer DL: **The interleukin-1 family of cytokines and receptors in human breast cancer: implications for tumor progression**. *International journal of oncology* 2003, **23**(2):269-284.
38. Goswami CP, Nakshatri H: **PROGgene: gene expression based survival analysis web application for multiple cancers**. *Journal of clinical bioinformatics* 2013, **3**(1):22.
39. Yan W, Cao QJ, Arenas RB, Bentley B, Shao R: **GATA3 inhibits breast cancer metastasis through the reversal of epithelial-mesenchymal transition**. *The Journal of biological chemistry* 2010, **285**(18):14042-14051.
40. Ross-Innes CS, Stark R, Teschendorff AE, Holmes KA, Ali HR, Dunning MJ, Brown GD, Gojis O, Ellis IO, Green AR *et al*: **Differential oestrogen receptor binding is associated with clinical outcome in breast cancer**. *Nature* 2012, **481**(7381):389-393.
41. Knopfova L, Benes P, Pekarcikova L, Hermanova M, Masarik M, Pernicova Z, Soucek K, Smarda J: **c-Myb regulates matrix metalloproteinases 1/9, and cathepsin D: implications for matrix-dependent breast cancer cell invasion and metastasis**. *Molecular cancer* 2012, **11**:15.

42. Drabsch Y, Ramsay RG, Gonda TJ: **MYB suppresses differentiation and apoptosis of human breast cancer cells**. *Breast cancer research : BCR* 2010, **12**(4):R55.
43. Khramtsov AI, Khramtsova GF, Tretiakova M, Huo D, Olopade OI, Goss KH: **Wnt/beta-catenin pathway activation is enriched in basal-like breast cancers and predicts poor outcome**. *The American journal of pathology* 2010, **176**(6):2911-2920.
44. Huber AH, Nelson WJ, Weis WI: **Three-dimensional structure of the armadillo repeat region of beta-catenin**. *Cell* 1997, **90**(5):871-882.
45. Bauer A, Chauvet S, Huber O, Usseglio F, Rothbacher U, Aragnol D, Kemler R, Pradel J: **Pontin52 and reptin52 function as antagonistic regulators of beta-catenin signalling activity**. *The EMBO journal* 2000, **19**(22):6121-6130.
46. Yook JI, Li XY, Ota I, Fearon ER, Weiss SJ: **Wnt-dependent regulation of the E-cadherin repressor snail**. *The Journal of biological chemistry* 2005, **280**(12):11740-11748.
47. Ertel A, Dean JL, Rui H, Liu C, Witkiewicz AK, Knudsen KE, Knudsen ES: **RB-pathway disruption in breast cancer: differential association with disease subtypes, disease-specific prognosis and therapeutic response**. *Cell cycle* 2010, **9**(20):4153-4163.
48. Dai M, Al-Odaini AA, Fils-Aime N, Villatoro MA, Guo J, Arakelian A, Rabbani SA, Ali S, Lebrun J: **Cyclin D1 cooperates with p21 to regulate TGFbeta-mediated breast cancer cell migration and tumor local invasion**. *Breast cancer research : BCR* 2013, **15**(3):R49.
49. Zhou F, Drabsch Y, Dekker TJ, de Vinuesa AG, Li Y, Hawinkels LJ, Sheppard KA, Goumans MJ, Luwor RB, de Vries CJ *et al*: **Nuclear receptor NR4A1 promotes breast cancer invasion and metastasis by activating TGF-beta signalling**. *Nature communications* 2014, **5**:3388.
50. Mantovani A, Allavena P, Sica A, Balkwill F: **Cancer-related inflammation**. *Nature* 2008, **454**(7203):436-444.

Supplementary Data

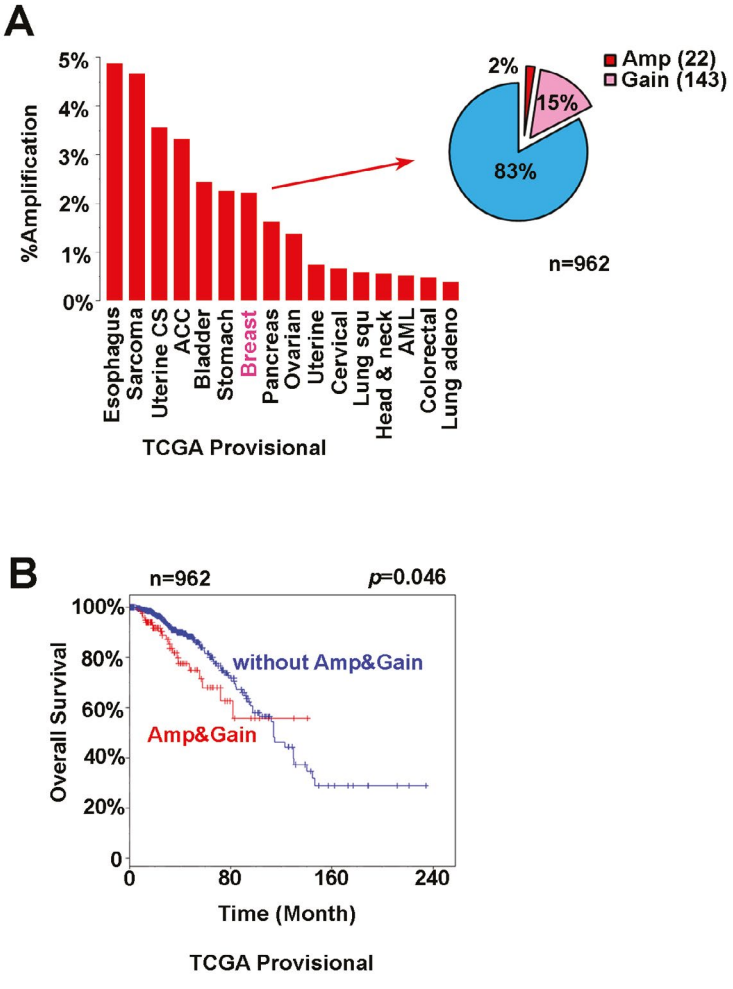

Figure S1. Copy number alterations of c-Myb in human breast cancer. A, Percentage of c-Myb amplifications in different human cancers. Data were analyzed by cBioportal from the TCGA dataset. B, Overall survival analysis of patients with breast cancer with or without c-Myb amplification and gain in the TCGA breast cancer dataset.

Figure S2

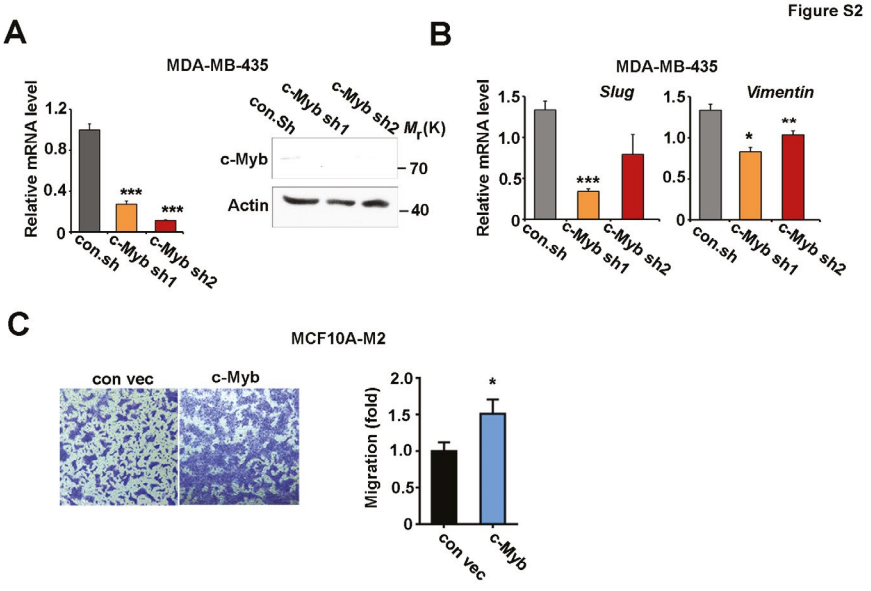

Figure S2. c-Myb is critical for breast cancer. A, MDA-MB-435 cells tably expressing control shRNA, or two independent shRNAs targeting c-Myb, were subjected to qPCR for c-Myb mRNA detection (left) or immunoblotting for c-Myb protein (right). The mRNA levels were normalized to GAPDH expression. mean ± s.d. of triplicates, ***p<0.001. B, qPCR analysis of mRNA levels of *Slug* and *Vimentin* in control or c-Myb depleted MDA-MB-435 cells. The levels were normalized to GAPDH expression. mean ± s.d. of triplicates, *p<0.05 **p<0.01 ***p<0.001. C, Left, Transwell migration assay of control and c-Myb overexpressing MCF10A-M2 cells. Right, fold changes of migrated cell numbers, mean ± s.d. .

Figure S3

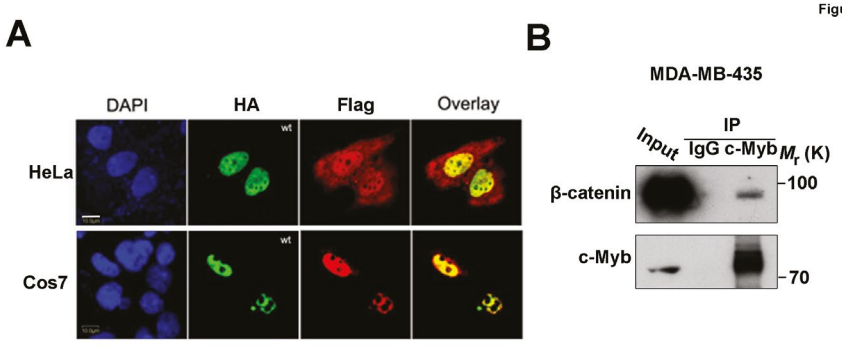

Figure S3. c-Myb interacts with β-catenin. A, HeLa and Cos7 cells were transfected with HA-c-Myb and Flag-β-catenin SA (a stable mutant) then stained with HA and Flag antibodies or DAPI. Confocal images display the nuclear staining of c-Myb (green) and the stableβ-catenin (red). scale bar: 10 μm. B, Interaction between endogenous c-Myb and β-catenin was detected by immunoblotting of Co-IP samples in MDA-MB-435 cells.

Table S1: Information of grading breast cancer tissue microarray

	Total		c-Myb					AXIN2				
			Low expression		High expression			Low expression		High expression		
	N	%	N	%	N	%	p-value	N	%	N	%	p-value
Age (years)												
<40	17	9.7	4	6.3	13	11.5	0.694	3	9.4	14	9.7	0.626
40-50	46	26.1	16	25.4	30	26.5		10	31.2	36	25.0	
50-60	49	27.8	18	28.6	31	27.4		6	18.8	43	29.9	
>=60	64	36.4	25	39.7	39	34.5		13	40.6	51	35.4	
Histological type												
Ductal	130	73.9	50	83.3	80	76.2	0.404	25	80.6	105	78.4	0.040
Lobular	18	10.2	4	6.7	14	13.3		6	19.4	12	9.0	
Other	28	15.9	6	10.0	11	10.5		0	0	17	12.7	
T-stage												
T1	100	57.5	31	49.2	69	62.2	0.220	19	59.4	81	57.0	0.648
T2	63	36.2	28	44.4	35	31.5		10	31.2	53	37.3	
T3/4	11	6.3	4	6.3	7	6.3		3	9.4	8	5.6	
N-stage												
N0	106	63.1	45	72.6	61	57.5	0.051	19	61.3	87	63.5	0.818
N1-3	62	36.9	17	27.4	45	42.5		12	38.7	50	36.6	
ER												
Negative	39	26.2	18	32.7	21	22.3	0.164	5	17.9	34	28.1	0.267
Positive	110	73.8	37	67.3	73	77.7		23	82.1	87	71.9	
PR												
Negative	57	38.5	26	48.1	31	33.0	0.068	9	32.1	48	40.0	0.442
Positive	91	61.5	28	51.9	63	67.0		19	67.9	72	60.0	
Her2												
Negative	55	82.1	16	76.2	39	84.8	0.395	9	81.8	46	82.1	0.980
Positive	12	17.9	5	23.8	7	15.2		2	18.2	10	17.9	

Supplementary material and methods

Plasmid lentiviral transduction

Lentiviral vectors were obtained from Sigma-Aldrich (MISSION®) for human c-Myb and Axin2 knockdown (shRNA TRCN0000040059, TRCN0000040062 and TRCN0000078539, respectively), as well as control vectors (pLV, pLKO-1). The lentiviral vectors that expressed c-Myb were generated by inserting the full-length human c-Myb cDNA fragments into pLV.CMV.bc.puro.

Lentiviral plasmids and 3 helper plasmids (pCMV-VSVG, pMDLg-RRE (gag/pol) and pRSV-REV) were co-transfected into HEK293T cells for lentivirus production. Cell supernatants containing the virus were harvested 48 h after transfection and stored at -80°C.

For generating stable cell lines, cells were infected at 20% confluence with lentiviral supernatants with normal culture medium (120 ng/ml of virus) in the presence of 8 ng/ml polybrene (Sigma) for 24 h. Then the cells were cultured under puromycin (1 μg/ml) selection.

RNA isolation and real-time qPCR

RNA was isolated using the NucleoSpin RNA II kit (BIOKE) followed by reverse transcription PCR (RevertAid First Strand cDNA Synthesis Kits, Fermentas). The cDNAs were analysed by real-time quantitative PCR (qPCR), and calculations were performed using the CFX Manager software version 2.0 (Bio-Rad). All mRNA expression levels were analysed in triplicate and normalized to *GAPDH* expression. The primer sequences are listed below.

GAPDH Forward: 5'-AGCCACATCGCTCAGACA C-3'

GAPDH Reverse: 5'-GCCCAATACGACCAAATC C-3'

N-cadherin Forward: 5'-CAGACCGACCCAAACAGCAAC-3'

N-cadherin Reverse: 5'-GCAGCAACAGTAAGGACAAACATC-3'

Snail Forward: 5'-ACCACTATGCCGCGCTCTT-3'

Snail Reverse: 5'-GGTCGTAGGGCTGCTGGAA-3'

Slug Forward: 5'-ATGAGGAATCTGGCTGCTGT-3'

Slug Reverse: 5'-GAGGAGAAAATGCCTTTGGA-3'

Vimentin Forward: 5'-CCAAACTTTTCCTCCCTGAACC-3'

Vimentin Reverse: 5'-CGTGATGCTGAGAAGTTTCGTTGA-3'

Twist Forward: 5'-GGAGTCCGCAGTCTTACGAG-3'

Twist Reverse: 5'-TCTGGAGGACCTGGTAGAGG-3'

Axin2 Forward: 5'-ATTCGGCCACTGTTCAGACG-3'

Axin2 Reverse: 5'-GACAACCAACTCACTGGCCTG -3'

Cyclin D1 Forward: 5'-TCAAGTGTGACCCGGACTGCCT -3'

Cyclin D1 Reverse: 5'-GCACGTCGGTGGGTGTGCAA-3'

Chromatin immunoprecipitation assay

Cells were fixed in 1% formaldehyde for 15 min at room temperature and then quenched by 5 min of treatment with 0.125 M glycine. Cells were harvested into ChIP lysis buffer (1% SDS, 50 mM Tris, pH 8.0, 5 mM EDTA and proteinase inhibitors) and sonicated to generate DNA fragments (200–400 bp). After centrifugation for 10 min at 14,000 rpm, the supernatant was diluted with dilution buffer (20 mM Tris pH 8.0, 2 mM EDTA, 1% Triton X-100, 150 mM NaCl, proteinase inhibitors) and then incubated overnight at 4°C with 3 μg of antibodies. Input samples were obtained before adding antibodies. The next day, 50 μl of protein A beads were added and the samples were incubated for 1 h at 4°C. The precipitates were pelleted and washed stepwise as follows: buffer TSE I (0.1% SDS, 20 mM Tris pH 8.0, 2 mM EDTA, 1% Triton X-100, 150 mM NaCl, proteinase inhibitors), TSE II (0.1% SDS, 20 mM Tris pH 8.0, 2 mM EDTA, 1% Triton X-100, 500 mM NaCl, proteinase inhibitors), LiCl buffer (10 mM Tris pH 8.0, 1 mM EDTA, 0.25 mM LiCl, 0.1% NP-40, 1% deoxycholate sodium) and TE (10 mM Tris, pH 8.0, 1 mM EDTA, pH 8.0). Elution buffer (400 μl; 25 mM Tris, pH 8.0, 10 mM EDTA, 0.5% SDS) was used to elute the bound immunocomplexes by incubation with vortexing at 65°C for 15 min. All samples were incubated with RNaseA (Thermo) and proteinase K (Thermo) at 65°C for 6–10 h to reverse the cross-linking and for purification. Two antibodies were used for the ChIP assay: anti-c-Myb (12319s, Cell Signaling) and anti-β-catenin (610154, BD Transduction Laboratories). All of the samples were measured by qRT-PCR. The primer sequences are listed below.

Actin promoter Forward: 5'- CTCTGACCTGAGTCTCCTT-3'

Actin promoter Reverse: 5'- GAGCCAGTGTTAGTACCTAC -3'

Axin2 promoter TCF binding Forward:

5'- AAGAAATCAGAACTCGGGC -3'

Axin2 promoter TCF binding Reverse:
5'- CCAGGACCTTATCAAAGCG -3'
Cyclin D1 promoter TCF binding Forward:
5'- GGGCTTTGATCTTTGCTTAAC -3'
Cyclin D1 promoter TCF binding Reverse:
5'- TGGAGGCTCCAGGACTTT-3'
Axin2 promoter c-Myb binding1 Forward:
5'- GGGACTTTGGAAGAGTAACG -3'
Axin2 promoter c-Myb binding1 Reverse:
5'- GCCTGAGTGCTAACACCAGT -3'
Axin2 promoter c-Myb binding2 Forward:
5'- AATGCTGGGATTACAGGC -3'
Axin2 promoter c-Myb binding2 Reverse:
5'- CACAACCTTCTCTTCTCCGT -3'

Transwell migration assay

A total of 5×10^4 cells were cultured in DMEM with 10% FBS and seeded in the upper compartment of 24-well polyethylene terephthalate inserts (Falcon, 8.0-μm pore size). After 16 hours of culture, cells migrated to the lower side of the insert filter. For analysis, cells remaining on the upper side of the membrane were removed, and cells on the lower side of the filter were fixed in 4% paraformaldehyde. After staining with 0.5% crystal violet, the migrated cells were counted and photographed. All experimental groups were assayed in triplicate wells.

Zebrafish xenograft assay

We performed a duct of Cuvier (DoC) injection to implant approximately 400 red-fluorescence labelled breast cancer cells into the circulation of transgenic zebrafish line Tg(fli1:GFP) embryos at 48 hpf. The Cell tracker CM-DiI(C-700, invitrogen) was used for MCF10A-M2 cells red fluorescence labelling. After the injection, zebrafish embryos were selected and maintained at 33°C for 6 days. All data are representative of at least 3 independent experiments with at least 50 embryos per group. Zebrafish maintenance and handling were approved by the Institutional Committee for Animal Welfare at the

Leiden University Medical Center (LUMC).

Animals and surgical procedures

Control or c-Myb depleted MDA-MB-231-luc (BM) cells were harvested in PBS. Five-weeks-old female Balb-c nu/nu mice were anaesthetized with isofluorane and 1×10^5 freshly cells were injected into the left heart ventricle (n=10 per group). Metastasis was detected weekly by BLI with the IVIS 100 (Caliper Life Sciences, Hopkinton, MA, USA). The BLI signal intensity was quantified as the sum of photons within a region of interest given as the total flux (photons/second). 5 weeks after injection, all mice were sacrificed and metastasis were analysed. All mice experiments were performed according to the guidelines for the care and use of laboratory animals in Zhejiang University.

Immunohistochemical staining and evaluation

We used antibodies against c-Myb (05-175, Merck Millipore) and Axin2 (ab32197, Abcam) for immunohistochemical staining. The tissue microarray (TMA) were conducted from breast cancer patients diagnosed and treated in the Leiden University Medical Center (LUMC) between 1996 and 2006. All sections were deparaffinized and rehydrated, and placed in 0.3% hydrogen peroxide methanol for 20 min to block endogenous peroxidase. Then slides were boiled in 10 mM sodium citrate buffer (pH 6.0) for antigen retrieval. After cooling down, sections were incubated overnight with either c-Myb (1:300) or Axin2 (1:2000) antibodies. This was followed by a 45 min incubation with biotinylated secondary mouse or rabbit antibody (DAKO), and 30 min ABC reagent incubation to amplify the target antigen signal. Sections were visualized in diaminobezidine solution, counterstained with haematoxylin. dehydrated, and mounted in malinol.

Microscopic analysis of c-Myb and Axin2 expression was performed by two independent observers in a blinded manner. The scores of the three punches were averaged. The percentage of positive nuclear staining (c-Myb) or the intensity of cytoplasmic staining (Axin2) were determined. For c-Myb a cut-off of 50% was used to define low (<50%) or high (>=50%) expression. For Axin2 no or weak staining intensity was defined as low Axin2 expression, and moderate or high staining intensity as high Axin2 expression.

Online clinical datasets

Figure 1A was analysed from oncomine. Data for Figure 1F and1G were downloaded from the Gene Expression Omnibus (GSE2990). To analyse genes correlation in Figure 3A, the original TCGA gene expression data were obtained from the Cancer Genome Atlas (https://tcga-data.nci.nih.gov); R software was used to calculate genes expression profile and correlation of 534 breast cancer patients. Data in Figure S1A,b were analysed from cBioportal (http://www.cbioportal.org). Data in Figure 7D were calculated by using PROGgene (http://watson.compbio.iupui.edu/chirayu/proggene).